Experimental Results for a CW-Mode Optically Controlled Microwave Switch with a Carrier-Confinement Structure

Sangil Lee, Yasuo Kuga and Ruth Ann Mullen

Department of Electrical Engineering, University of Washington, Box 352500

Seattle, WA 98195-2500, USA

Abstract — **A new design for a CW-mode optically controlled microwave switch (CW-mode OMS) on a semiconductor coplanar waveguide (CPW) is investigated, which is based on a silicon (Si) substrate etching for both top and bottom to confine the optically generated free-carriers. We fabricate the CW-mode OMS with and without carrier-confinement structures using a micro-fabrication technique, and the insertion loss is measured and compared. With the new carrier-confined CW-mode OMS, we are able to obtain less than 2 dB of insertion loss which is an improvement of more than 5 dB from without the carrier-confinement structure. Also, more than 20 dB of the ON/OFF difference is obtained up to 20 GHz.**

I. INTRODUCTION

There has been an increasing interest in the photo-conductivity effect to control microwave solid-state devices which offers several advantages, such as fast response, immunity from electromagnetic interference, high power handling, good isolation between controlling and controlled devices, and possibilities for monolithic integration [1]. One of the basic applications for the photoconductivity effect as a switch is a direct excitation of the gap on a semiconductor transmission line using a laser light source. Thus, the transmission characteristics can be controlled by the amount of optically generated free-carriers, which can be used for a switching device or an attenuator.

Initial studies on OMS employed pulse-mode microwave devices using picosecond laser sources [2]. Later, CW-mode optically controlled microwave devices were developed for switches and attenuators. With the CW illuminations, the loss of optically generated free-carriers due to recombination and carrier diffusion cannot be ignored. Although the CW-mode microwave switching devices have been investigated analytically and experimentally [3]-[5], the best-case insertion loss in the CW-mode operation has not been tested. Unlike pulse-mode photoconductivity devices, there are limitations in improving the insertion loss of the CW-mode OMS only with an increase of the incident optical power. Based on our experiments, it was very difficult to obtain less than 7 dB of insertion loss with a standard CPW structure having a 25 μm gap at a frequency range 0.5 to 20 GHz [6]. This may suggest that the CW-mode OMS requires a proper carrier-confinement technique to obtain better insertion loss.

In pulse-mode OMS, the recombination rate is not an important factor. Thus, a direct bandgap material such as GaAs can be effectively used to reduce the switching speed. However, in the CW-mode operation, the number of optically generated free-carriers is directly related to the recombination rate of the substrate material. In the steady state, the number of optically generated free-carriers is given by [7]

$$\Delta n = \frac{\alpha I(\omega)}{h\omega}(1-R)S\tau \qquad (1)$$

where α is the absorption coefficient, $I(\omega)$ is light intensity, $h\omega$ is the photon energy to excite electrons, R is the surface reflectivity, S is the relative spectral response of the semiconductor material exhibiting a peak response at λ_0 and τ is the recombination rate or a carrier life time. Although (1) neglects some phenomena such as carrier diffusion and surface recombination, it provides a critical point for the selection of a substrate material. In general, a substrate with a longer lifetime can maintain a higher free-carrier density at the expense of switching speed. This will restrict the choice of the substrate material to an indirect bandgap material such as a Si wafer for the CW-mode operation, and the diffusion length of the optically generated free-carriers will be getting longer with a longer life time. Thus, it is expected that the physical confinement of the free-carriers will be important to improve the insertion loss, which can be done by Si substrate etching.

II. DESIGN AND FABRICATION

The basic confining idea is to make grooves around the gap area, which can be implemented by Si substrate etching. Fig. 1 shows a proposed groove design. The groove patterns are two separated regions. One pattern is located between the ground plane and the signal line around the gap area (dark gray) and the other pattern is on

0-7803-7239-5/02/$10.00 © 2002 IEEE

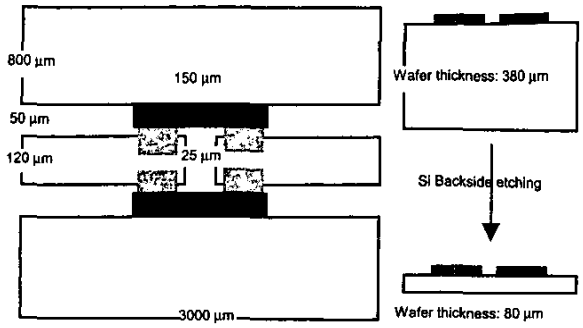

Fig. 1. A new carrier-confined OMS with etching patterns.

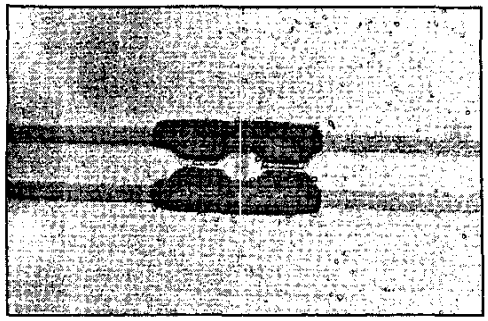

Fig. 2. A picture of the fabricated sample with a carrier-confinement structure.

the signal line (bright gray). The most effective way to confine the carriers is an encapsulation of the exciting area with the air gap by the substrate etching, but it may not be a possible process without the disconnection of the signal line. Thus, we can make etching patterns only partially on the signal line for further confinement. If we make a narrower signal line, we can confine more carriers, but there will be more reflections at the narrower signal line due to impedance change especially at the high frequency range. However, numerical simulation results showed that the loss due to the narrower signal line was less than 0.5 dB, which may not be significant. Another way to confine the carriers is to minimize the substrate thickness. The thickness of the Si wafers we use is approximately 380 μm. Although we confine the carriers horizontally, there is large space to diffuse out to the bottom. Thus, it is expected that a thinner substrate can confine the carriers more effectively. The thinner substrate can be made with the backside etching of the substrate after the final process step. However, less than 50 μm will be too thin to handle the next step based on our experience. Fig. 2 shows a picture of the fabricated sample. The actual etching areas are larger than the designed areas. We use a dry etching technique with a Trion RIE, which has under cutting problems due to the isotropic Si etching. Therefore, this under cutting problem should be considered in the etching pattern design.

A simple micro-fabrication technique is applied to make the CPW line patterns and groove patterns on a high-R (~ 5000 Ω.cm) Si wafer. Cr and Au are deposited for 200 A° and 5000 A°, respectively, using an E-beam evaporator. A metal wet-etching technique is used for obtaining the CPW line patterns. Then, the second photolithography for the etching pattern and the RIE Si etching is conducted. A thin silicon dioxide layer on a Si wafer reduces the surface recombination rate, which may increase the number of generated free-carriers. However,

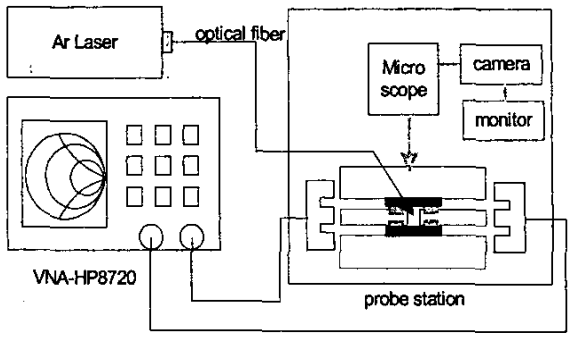

Fig. 3. Measurement setup.

there may be a heat dissipation problem with a thick silicon dioxide layer. Thus, the silicon dioxide layer is thermally deposited before the device fabrication to observe the effect of the silicon dioxide thickness.

Fig. 3 shows the measurement setup. An Ar laser (λ= 488 nm) is used for an incident optical power, and the light is guided through the multi-mode optical fiber. The maximum optical power at the tip of the fiber is approximately 30 mW. The transmission characteristics are measured with a vector network analyzer (HP8720D) and a 3D microwave probe station at a frequency range from 500 MHz to 20 GHz.

III. Measurement Results

Several samples are fabricated and tested to observe the carrier-confinement effect with the new design and the silicon dioxide thickness effect. All the measurements are *'Thru'* calibrated with a reference line having no gap, and

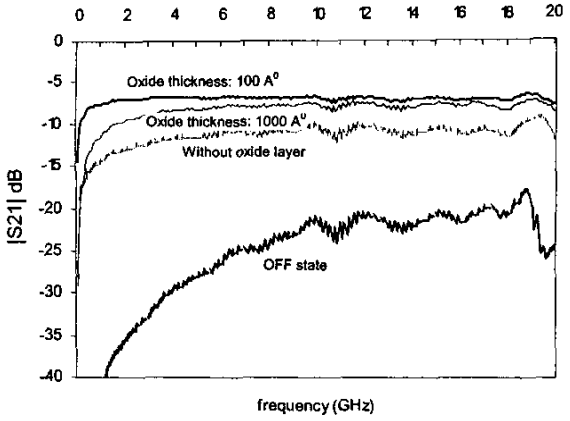

Fig. 4. Insertion loss measurements for a different silicon dioxide thickness at 6 mW.

the insertion loss can be read directly from the plot. Fig. 4 shows the measured insertion loss for a different silicon dioxide thickness as a function of frequency at 6 mW incident optical power. As shown in Fig. 4, a thin oxide layer improves the insertion loss, but the improvements depend on the layer thickness. With the measurements, the silicon dioxide thickness is optimized around 100 A^0.

Fig. 5 shows both insertion loss (a) and ON/OFF difference (b) with and without carrier-confinement structure as a function of frequency at 20 mW incident optical power. As shown in Fig. 5, both insertion loss and ON/OFF ratio are significantly improved with the carrier-confinement structure and a thin silicon dioxide layer. Each groove pattern on top of the substrate improves the insertion loss less than 1 dB because the improvements include the effect due to the thin silicon dioxide layer. Rather, substrate etching reduces the insertion loss more substantially. Fig. 6 shows the insertion loss as a function of incident optical power at 6 GHz. The insertion loss is decreased linearly with the higher optical power up to 5 mW, and it is saturated at approximately 20 mW. Finally, less than 2dB of insertion loss and better than 20 dB of the ON/OFF difference are obtained with the new carrier-confinement structure and a thin silicon dioxide layer.

IV. Numerical Simulations

To analyze the experimental results, the transmission characteristics of the CW-mode OMS are simulated in terms of the effective photoconductivity and the effective plasma depth of the gap region [3] with the finite element code HFSS (High Frequency Structure Simulator). The maximum number of optically generated free-carriers on the surface in the steady state can be obtained from (1), which does not consider the carrier diffusion, and the

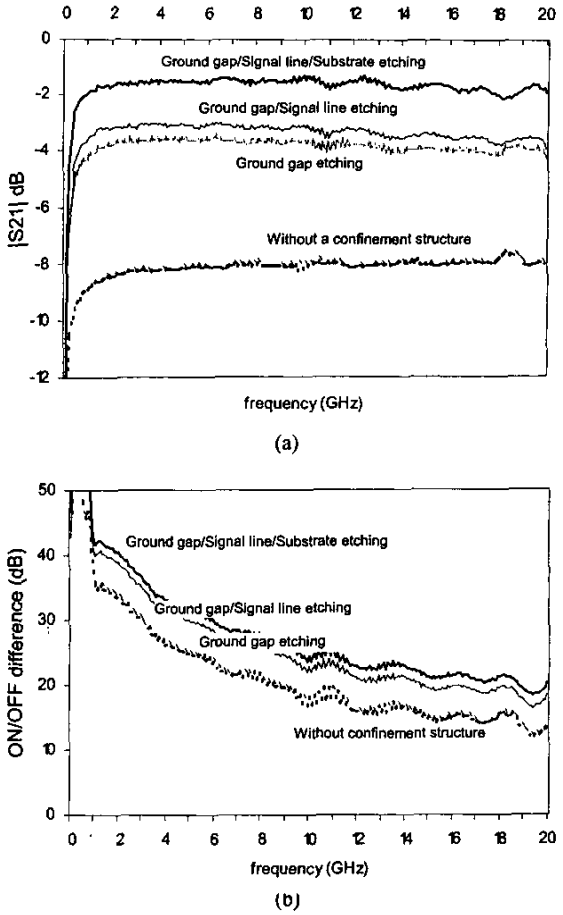

Fig. 5. Carrier-confinement structure measurements as a function of frequency at 20 mW (a) insertion loss (b) ON/OFF difference

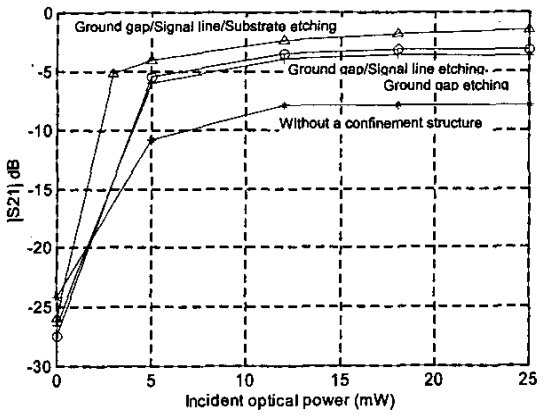

Fig. 6. Carrier-confinement structure measurements as a function of incident optical power at 6 GHz: Insertion loss

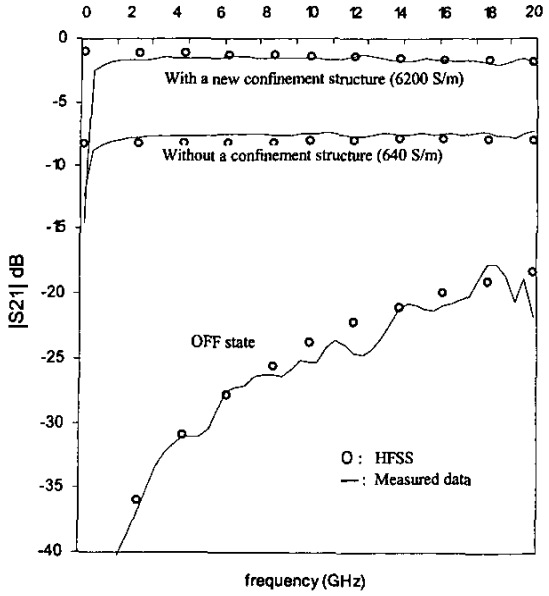

Fig. 7. HFSS simulation results for insertion loss compared with the measured data.

photoconductivity due to the optically generated free-carriers is expressed by

$$\Delta\sigma_o = q\Delta n(\mu_n + \mu_p) \qquad (2)$$

where q is the electrical charge, Δn is the number of optically generated free-carriers, and μ_n and μ_p are the mobilities of electrons and holes, respectively. We suppose that the effective photoconductivity of the gap region ($\Delta\sigma_{eff}$) is the same as $\Delta\sigma_o$ for $1/\alpha$ from the surface. Then, the $\Delta\sigma_{eff}$ becomes 5 x 10^6 S/m with 88 W/cm^2 of the incident optical power density which corresponds 10 mW with 120 μm beam diameter, and the effective plasma depth is 1 μm. This shows that the gap becomes a good conductor if the carrier diffusion can be ignored. Other quantities used for the calculation are: $\alpha = 1\times10^4$ cm^{-1}, $\tau = 10^{-4}$ sec, *S=0.5*, *R=0.3*. As expected, close to 0 dB of the insertion loss is obtained from the HFSS simulations with $\Delta\sigma_{eff}$ =5 x 10^6 S/m.

Although a carrier diffusion is considered, and the plasma depth is getting longer, the photoconductivity around the surface area is still an important factor for the insertion loss. Thus, the effective photoconductivity for the 3 μm from the surface as an effective plasma depth is obtained from the measured insertion loss and the HFSS simulations. Both HFSS simulation results and the measured insertion loss are shown in Fig. 7. From the comparison, it is estimated that the effective conductivities are 6200 S/m and 640 S/m for with and without carrier confinement structure, respectively, at 20 mW. Therefore, approximately 10 times higher effective photoconductivity is obtained with the new carrier- confinement technique.

V. Conclusion

The best-case insertion loss has been measured for the CW-mode OMS with a new carrier-confinement structure, which is implemented by the Si substrate etching around the gap area. Without a carrier-confinement structure, it has been very difficult to obtain less than 7 dB of the best-case insertion loss with maximized optical power. However, the new carrier confinement structure improves the insertion loss more than 5 dB. Finally, we have obtained less than 2 dB of insertion loss and better than 20 dB of the ON/OFF difference with the new design. Also, approximately 10 times higher effective photoconductivity has been achieved for the effective plasma depth with the HFSS simulations.

Acknowledgement

This work was supported by the National Science Foundation (grant ECS-9908849) and the U.S. Office of Naval Research (grant N00014001027).

References

[1] C. H. Lee, "Picosecond optics and microwave technology," *IEEE Trans. Microwave Theory and Tech.*, vol. MTT-38, no. 5, pp. 596-607, May 1990.

[2] A. M. Johnson, and D. H. Auston, "Microwave switching by picosecond photoconductivity," *IEEE J. of Quantum Electronics*, vol. QE-11, no. 6, pp. 283-287, June 1975.

[3] W. Platte, "Effective photoconductivity and plasma depth in optically quasi-CW controlled microwave switching devices," *IEE Proceedings*, vol. 135, Pt. J, no. 3, June 1988.

[4] W. Platte, and B. Sauerer, "Optically CW-induced losses in semiconductor coplanar waveguides," *IEEE Trans. Microwave Theory and Tech.*, vol. MTT-37, no. 1, pp.139-149, January 1989.

[5] D. A. M. Khalil, and A. M. E. Safwat, "On the improvement of the performance of the optically controlled microwave switch," *IEEE Trans. Microwave Theory and Tech.*, vol. MTT-45, no. 8, pp. 1358-1361, August 1997.

[6] S. Lee, and Y. Kuga, "Optically CW-mode controlled microwave switches with carrier-confinement on a coplanar waveguide," *2001 IEEE Antennas & Propagation Society Int. Symp. Dig.* vol. 2, pp. 514-517, July 2001.

[7] M. A. Omar, *Elementary Solid State Physics*, pp. 302-304 Addison-Wesley Publishing Company, Inc. 1975.